AIAA-2003-4701

Modeling of the Plasma Flow in High-Power TAL

Michael Keidar, Iain D. Boyd and Javier Parrilla

Department of Aerospace Engineering, University of Michigan, Ann Arbor MI 48109

Abstract

Recently great emphasize was put forward into high power Hall thruster development. Among Hall thruster technologies, the thruster with anode layer (TAL) seems to have much wider technical capabilities. In this paper, various aspects of the plasma flow in a high power thruster with anode layer are studied. A model of plasma flow in the TAL channel is developed based on a 2D hydrodynamic approach. In particular, plasma –wall interactions are studied in detail. Formation of the sheath near the acceleration channel wall and sheath expansion in the acceleration channel are calculated. Both single- and two-stage TALs are investigated. It is found that the high voltage sheath expands significantly and the quasi-neutral plasma region is confined in the middle of the channel. For instance, in the case of a 3 kV discharge voltage, the sheath thickness is about 1 cm, which is a significant portion of the channel width. An effect of sheath expansion on the acceleration region is studied using a quasi 1D simplified model. It is found that sheath expansion decreases the acceleration region length. The single stage, high voltage TAL (D-80) is studied. The model predicts a non-monotonic behavior of thruster efficiency with discharge voltage. The location of maximum efficiency is found to be in agreement with experiment.

I. Introduction

Hall thrusters are among the most advanced and efficient types of electrostatic propulsion devices. The Hall thruster configuration is beneficial because the particle acceleration takes place in a quasi-neutral plasma and thus is not limited by space charge effects. The electrical discharge in the Hall thruster occurs across the external magnetic field which has a predominantly radial component and ions are accelerated along the axial electric field. Passing the electron current across a magnetic field leads to an electron closed drift or Hall drift, that provides the necessary gas ionization. The original idea of ion acceleration in the quasi-neutral plasma was introduced in the mid 60's (see Refs. 1,2,3,4) and since then numerous experimental and theoretical investigations have been conducted. The main results of these studies were summarized in recent reviews[5,6]. Generally two different types of Hall thruster were developed: a thruster with closed electron drift and extended acceleration zone, or Stationary Plasma Thruster (SPT), and a thruster with short acceleration channel or Thruster with Anode Layer (TAL). In a SPT, the interaction of the plasma with the dielectric wall plays an important role. Due to the collisions of the electrons with the wall and secondary electron emission, the electron temperature remains relatively low in comparison to the TAL. As a result, the ion acceleration occurs over a more extended region[4,7]. On the other hand in a TAL, the ion acceleration takes place over a very short length of about the electron Larmor radius. Despite many theoretical efforts, the complicated physical processes in the Hall thruster channel are far from being completely understood. Mainly the physics of the electron transport, plasma interaction with the wall, and the transition between the quasi-neutral plasma and the sheath have not been investigated in detail.

In the TAL variant, an electric discharge in the crossed magnetic and electric fields is created in the gap between magnetic poles where closed electron drift takes place. In this gap, the neutral atoms are ionized and accelerated. Some fraction of the accelerated ion stream is directed toward the wall that limits the

discharge in the radial direction and protects the magnetic poles from erosion. This leads to wear of these walls due to ion bombardment and results in a shorted lifetime of such accelerators.

Recently great emphasize was put into development of high power Hall thrusters[8]. Among Hall thruster technologies, the TAL configuration seems to have much wider technical capabilities and range of parameters.[9] Being that reduced erosion of the various parts, such as electrodes, insulators, screens, etc. is critical for the long term operation of the thruster, the TAL variant of the Hall thruster technology seems to be beneficial since it has a very small acceleration region and therefore small area with contact of ions with materials were possible erosion occurs. In order to meet high power requirements, a thruster with anode layer (TAL) was developed and an experimental model was presented.[10] TAL using Bismuth as a propellant demonstrated specific impulse in the range of 2000-5000s at the power level of 10-34 kW.

In the TAL, ions are accelerated in a very short region, which is about an electron Larmor radius and in which almost the entire voltage drop is concentrated. It should be noted that this idealized picture is not exact and in reality in the TAL as well as in some SPT's significant ion acceleration occurs outside of the channel in the fringing magnetic field. This may be considered as one possible mechanism of high plasma beam divergence in Hall thrusters[10]. While TAL's can operate in both single and two stage regimes, the two-stage regime of operation has many advantages, for instance the possibility to achieve much higher specific impulse.[11] When a two-stage thruster is considered, the most important region in terms of long time operation is the second acceleration stage in which a very large voltage drop is applied. The second stage channel geometry is shown schematically in Fig.1.

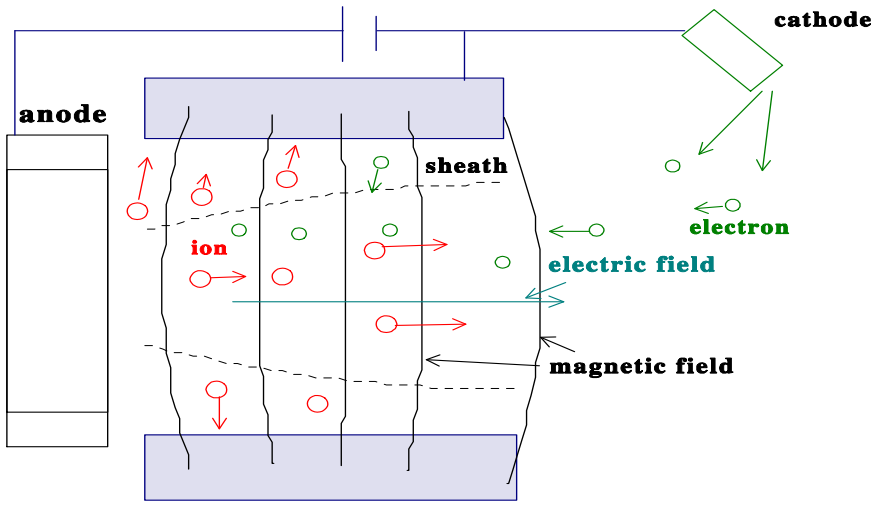

Figure 1. Schematics of the acceleration channel in a TAL

The plasma-wall transition region in the TAL channel determines the particle and energy fluxes from the plasma to the wall. Recently we presented a model of plasma wall transition that accounts for secondary electron emission[12]. In order to develop a self-consistent model, the boundary parameters at the sheath edge (ion velocity and electric field) are obtained from a two-dimensional plasma bulk model. In the considered condition, i.e. ion temperature much smaller than that of electrons and significant ion acceleration in the axial direction, the presheath scale length becomes comparable to the channel width so that the plasma channel becomes an effective presheath. It was shown that a plasma-sheath matching approach proposed previously can be used.[13] In this approach, the electric field that develops in the presheath can serve as a boundary condition for the sheath. At the same time the model predicts that the quasi-neutrality assumption at the presheath edge is still valid.

II. Plasma-wall transition

It was shown (Ref. 12) that the presheath scale length becomes comparable to the channel width under typical conditions of the Hall thruster channel. Thus, the model for the quasi-neutral plasma region is extended up to the sheath edge in order to provide the boundary condition at the plasma-sheath interface as shown in Fig. 2.

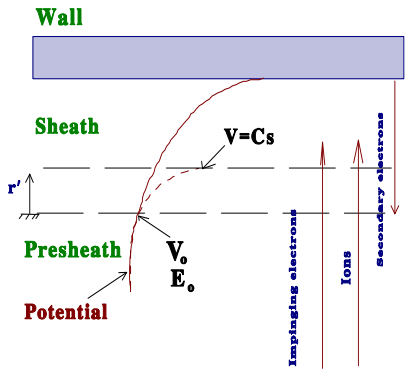

Figure 2*. Schematic of the plasma-wall transition layer. The boundary at r'=0 corresponds to smooth transition with monotonic potential behavior across the transition layer*

The smooth transition between sheath and presheath is considered in the present work following the methodology developed previously by Beilis and Keidar.[13] If the velocity at the sheath edge differs slightly from the Bohm velocity, the electric field becomes a continuous function. It was shown that a monotonic solution for the sheath problem could be obtained when the ion velocity at the sheath edge is smaller than the Bohm velocity[12,13]. In this case, the electric field becomes a continuous function increasing from a small non-zero value at the sheath edge up to a maximum value at the wall as shown schematically in Fig. 2. The solution criterion in that case is the minimal velocity at the presheath-sheath interface that results in a continuous solution for the potential distribution in the sheath. Previously we applied this approach to the plasma-wall interaction in a

SPT Hall thruster. It was shown that the ion velocity at the presheath edge increases with axial distance from about $0.7C_s$ up to C_s, where C_s is the sound speed.

In this paper we describe several models that we developed to study plasma flow in TALs, such as a 2D hydrodynamic model, which is used to study general features of the flow. In addition, to study effect of the sheath expansion we developed a simplified quasi-1D model.

III. Hydrodynamic model

The model is based on the assumption that the quasi-neutral region length (i.e. channel width, see Fig. 1) is much larger than the Debye radius and therefore we will assume that $Z_i n_i = n_e = n$, where Z_i is the ion mean charge, n_i is the ion density and n_e is the electron density. For simplicity only single charge ions are considered in this paper ($Z_i = 1$). We will consider the plasma flow in an annular channel as shown in Fig. 1. A magnetic field with only a radial component, $B_r = B$, is imposed. Cylindrical coordinates will be used with angle θ, radius r, and axial distance from the anode z, respectively. The plasma flow starts in the near anode region and has lateral boundaries near the dielectric wall. The plasma presheath-sheath interface is considered to be the lateral boundary for the plasma flow region. A plasma will be considered with 'magnetized' electrons and 'unmagnetized' ions, i.e. $\rho_e << L << \rho_i$, where ρ_e and ρ_i are the Larmor radii for the electrons and ions respectively, and L is the channel length. We employ a hydrodynamic model assuming: (i) the system reaches a steady state, and (ii) the electron component is not inertial, i.e. $(\mathbf{V}_e \nabla) \cdot \mathbf{V}_e = 0$.

Generally two regimes are possible in a TAL, the so called vacuum regime (in which the electron density is much higher than that of ions) and the quasi-neutral plasma regime.[14] Below, we briefly formulate a model for the quasi-neutral regime. A hydrodynamic model is employed in a 2-D domain assuming that

the system reaches a steady state. The momentum and mass conservation equations for electrons, ions and neutrals under these conditions have the following form:

$$nm_i(V_i\nabla)V_i = neE - \nabla P_i - \beta n m_i n_a (V_i - V_a) \quad (1)$$

$$0 = -en(E + V \times B) - \nabla P_e - n\nu_{ef} m_e V_e \quad (2)$$

$$\nabla \cdot (V_i n) = \beta n n_a \quad (3)$$

$$\nabla \cdot (V_a n_a) = -\beta n n_a \quad (4)$$

$$\frac{3}{2}\partial(j_e T_e)/\partial z = Q_j - Q_w - Q_{ion} \quad (5)$$

where i, a, e are subscribes for ions, neutral atoms and electrons, respectively, n is the plasma density, β is the ionization rate, V is the velocity, $Q_j = j_e E$ is the Joule heat, E is the axial component of the electric field, j_e is the electron current density, $Q_w = \nu_w n (2kT_e + e\Delta\varphi_w)$ represents the wall losses[12], ν_w is the frequency of electron collisions with walls, $Q_{ion} = en_a n U_i \beta$ represents ionization losses, U_i is the ionization potential (for Xenon, U_i=12.1 eV). To simplify the problem without missing the major physical effects, we consider one-dimensional flow of the neutrals. The equations for the heavy particles (ions and neutrals) may be written in component form in cylindrical coordinates by taking into account that the ion temperature is much smaller than the electron temperature (that makes it possible to neglect the ion pressure term in the momentum conservation equation):

$$\frac{\partial(nV_z)}{\partial z} + \frac{\partial(nV_r)}{\partial r} + \frac{nV_r}{r} = \beta n_i n_a \quad (6)$$

$$V_z \frac{\partial V_z}{\partial z} = -V_r \frac{\partial V_z}{\partial r} + \frac{e}{m_i} E_z - \beta (V_i - V_a) n_a \quad (7)$$

$$V_z \frac{\partial V_r}{\partial z} = -V_r \frac{\partial V_r}{\partial r} + \frac{e}{m_i} E_r \quad (8)$$

$$\frac{\partial(n_a V_a)}{\partial z} = -\beta n_i n_a \quad \text{..... (9)}$$

In this model the electron flow (Eq. 2) will be considered separately along and across magnetic field lines. Due to the configuration of the magnetic field (i.e. only the radial magnetic field component is considered in the model), the electron transport is greater in the azimuthal direction (E×B drift) than in the axial direction (drift diffusion due to collisions). According to Eq. 2, the electron transport equation along the magnetic field can be written as a balance between pressure and electric forces assuming that the current component in the radial direction is zero. If we assume that the electron temperature is constant along each magnetic field line we obtain that

$$\varphi - \frac{kT_e}{e} ln n = \text{const} \quad \text{..... (10)}$$

The left hand side of this equation is known as a thermalized potential[5]. This equation makes it possible to reduce the two-dimensional calculation of the electric field to a one-dimensional problem. According to Eq. 10 the electric field in the radial direction E_r is determined by the electron pressure gradient in this direction. Calculating the potential distribution along the channel centerline makes it possible to calculate the potential in the entire domain using Eq. 10, similar to Ref. 12. For known total discharge current and ion current fraction one can calculate the electron current fraction from the current continuity condition. The equation describing the electron transport across the magnetic field can be obtained from Eq. 2 and reads:

$$j_{ez} = en\frac{\mu_e}{1+(\omega_e/\nu_m)^2}\left(E_z + \frac{\partial T_e}{\partial z} + T_e\frac{\partial ln n}{\partial z}\right) \quad \text{..... (11)}$$

where $\nu_m = \nu_{en} + \nu_{ew} + \nu_B$ is the effective electron collision frequency. In the following we will determine different components of the effective electron collision frequency.

Electron collisions

For typical conditions of the Hall thruster, the effect of Coulomb collisions appears to be negligibly small[15] and will not be considered here. The total electron collision frequency considered in the present model consists of electron-neutral collisions and anomalous collisions (Bohm diffusion). The electron-neutral collision frequency may be estimated as follows:

$$\nu_{en} = n_a \sigma_{ea} V^e_{th} \quad \text{..... (12)}$$

where n_a is the neutral density, σ_{ea} is the collision cross section dependent on the electron energy[12] ($\sigma_{ea} \sim (10 \div 40) \times 10^{-20} m^{-2}$ for Xenon, in considered energy range), and V^e_{th} is the electron thermal velocity.

However, only including the classical mechanism of collisions cannot explain the electron transport observed in a Hall thruster. This was recognized long ago by many authors[5,6]. Until now, however, there is no consensus about which of the possible mechanisms of electron transport is most significant in the Hall thruster. While in the SPT electron collisions with the walls may play the major role[4], in the TAL, which does not have significant secondary electron emission anomalous transport[16] may be important. In the present work we will include anomalous (Bohm) transport. The effective electron collision frequency related to the anomalous transport (Bohm diffusion) can be estimated as

$$\nu_B = \alpha \omega_e \text{ , } \quad \text{..... (13)}$$

where $\alpha \sim 1/16$ is the Bohm empirical parameter in the classical formulation. It will be shown below that the exact value of this parameter affects the potential drop across the channel. The best fit with the experimental data of the potential drop for a given discharge current corresponds to $\alpha \sim 1/100$ instead of

the classical value ~1/16. It should be noted that the same conclusion derived by different authors was that the best fit with the experiment corresponds to α~1/80 to 1/100 (Ref. 12,17,18).

Boundary conditions

In order to obtain a solution of the system of equations (6)-(13) the following boundary conditions must be specified. At the upstream boundary (z=0) we specify the density and velocity similarly to Refs. 12,19 assuming sonic ion velocity near the anode plane. This upstream condition implies that we are considering only supersonic plasma flow assuming that the transition from subsonic to supersonic flow[24] occurs in the anode vicinity. The atom velocity near the anode is assumed to be $V_{oa}=2x10^2$ m/s (Ref. 15). The atom density at the anode plane depends upon the mass flow rate. At the downstream boundary (thruster exit plane, z=L) we specify an electron temperature of T_e=10 eV (Ref. 15).

Numerical method

The numerical analysis is similar to that developed previously[20]. We use the implicit two-layer method to solve the system of equations (6)-(10). These equations are approximated by a two layer six point scheme. The electron temperature distribution is calculated by iteration initially assuming a trial temperature distribution that satisfies the boundary conditions.

IV. High power Bismuth TAL

In this section we describe the model of a particular TAL design that uses Bismuth as the propellant. The Bismuth thruster was originally developed in the 1960's in the former USSR.[9] It was demonstrated that specific impulse in the range of 2000-5000 s at the power level of 10-34 kW can be achieved. This thruster has a two-stage configuration in order to separate the ion production and acceleration zones. The simulations correspond to the following case: discharge current I=6 A, mass flow rate is 20 mg/s, magnetic field is uniform and equals 0.2 T. The 2D hydrodynamic model described in the previous section is used to calculate plasma flow in the second stage channel.

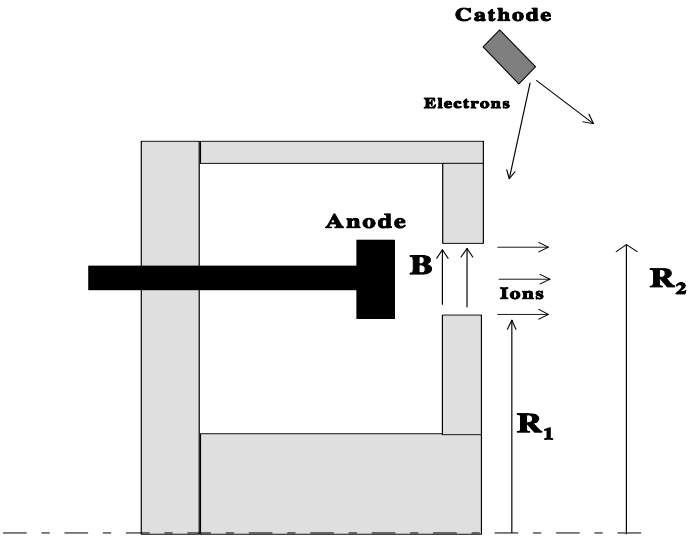

Figure 3. Schematic of the acceleration channel in a TAL

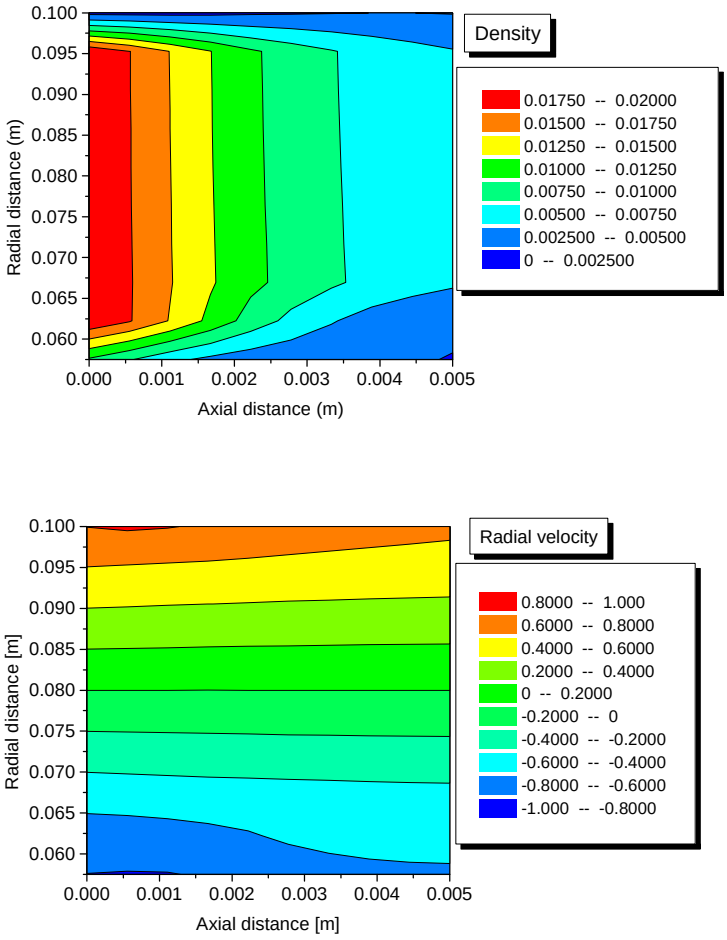

Figure 4. Density and velocity distribution along the channel

Computational domain is shown schematically in Fig.3. Plasma density (normalized by neutral density at the anode) and radial velocity (normalized by sound speed) distributions are shown in Fig.4. One can see that the radial velocity towards the channel walls is about 0.5 of the sound speed. It should be noted that this velocity as well as boundary plasma density determine the flux to the wall and therefore the wall erosion rate.

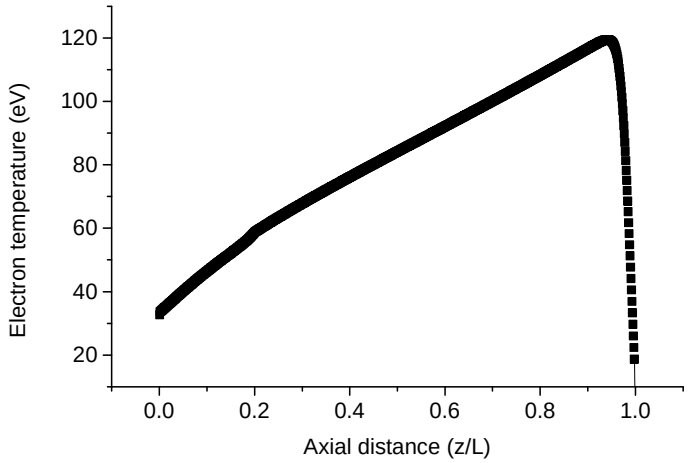

Figure 5. Electron temperature distribution in the acceleration channel of TAL

The electron temperature distribution along the channel is shown in Fig. 5. One can see that electron temperature peaks at about 120 eV near the channel exit plane and decreases towards the anode.

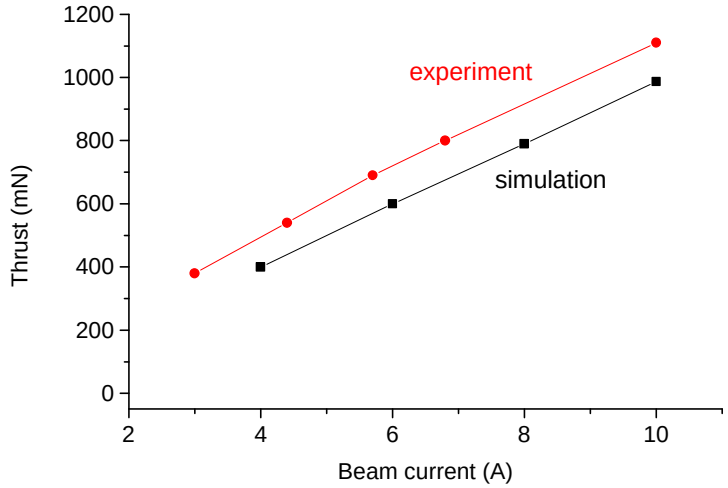

Fig. 6. Comparison of calculated and measured thrust (experimental data are taken from Ref. 9)

The calculated thrust linearly increases with the current (ion beam current) in agreement with experiment as shown in Fig. 6.

In the second stage channel, the guard ring has the cathode potential. When high voltage across the acceleration channel is considered, one should take into account the importance of the sheath development near the screening walls (guard ring) of the channel as shown in Fig. 3. When a negative voltage (cathode potential in considered case[9]) is applied to a surface immersed in a plasma, electrons are repelled from the surface, leading to sheath formation. Electrons drift away from the surface due to the presence of the high electric field. In the steady state, the ions are then accelerated toward the surface by the electric field of the sheath. In the one-dimensional steady state case the sheath thickness can be estimated according to the Child-Langmuir law:[21,22]

$$s = (\frac{4}{9}\varepsilon)^{1/2}(\frac{2Z_i e}{m_i})^{1/4}\frac{U^{3/4}}{(eZ_i NV)^{1/2}} \qquad (14)$$

where V is the ion velocity at the sheath edge, U is the voltage across the sheath, s is the sheath thickness, ε is the permittivity of vacuum, Z_i is the ion mean charge number, N is the plasma density at the sheath edge, and m_i is the ion mass. One can see that the steady-state sheath thickness is determined by plasma density and ion velocity at the sheath edge for a given bias voltage.

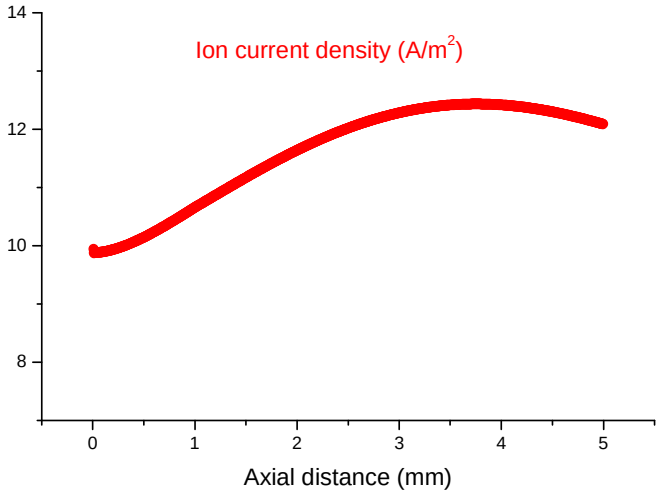

Figure 7. Ion flux to the wall along the acceleration channel in TAL. The acceleration voltage is 3 kV.

Based on the hydrodynamic model, the plasma parameters as well as ion flux to the wall is calculated. These results are shown in Fig.7. The sheath thickness is about 1 cm and occupies a significant portion of the channel (see Fig. 8). It is important to mention that when a higher power TAL is considered (and therefore higher acceleration voltage is applied) the ion energy as well as sheath thickness will increase. Considering the interaction of the high-energy ion flux with wall materials one can expect significant erosion. For instance, in the case of 3 kV acceleration voltage, the maximal erosion rate of an iron wall interacting with Xe ions would be on the order of 1000 μm after 300 h of operation.

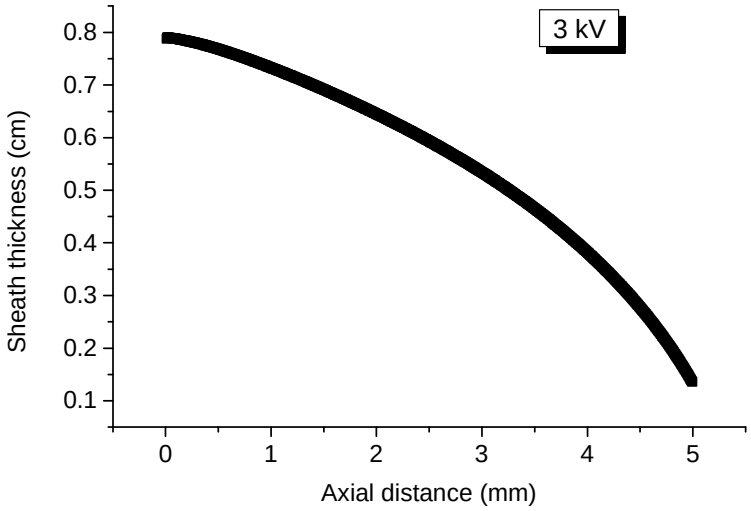

Fig. 8. Sheath thickness as a function of axial position.

V. High Voltage D-80 TAL

In this section another example of a TAL device is considered with respect to behavior in the high voltage regime: the D-80 TAL that was developed by TsNIMASH. In single stage configuration, the thruster was operated with discharge voltage ranging from 300 to 1700 V having specific impulse from 1630 to 4140 s. (Refs. 8,11) In this section, we describe the computational results for this particular thruster with the view to understand the experimentally observed effect of thruster efficiency drop at high voltages.

The calculations are performed for the following parameters: mass flow rate is 4 mg/s and the discharge current is 3 A.

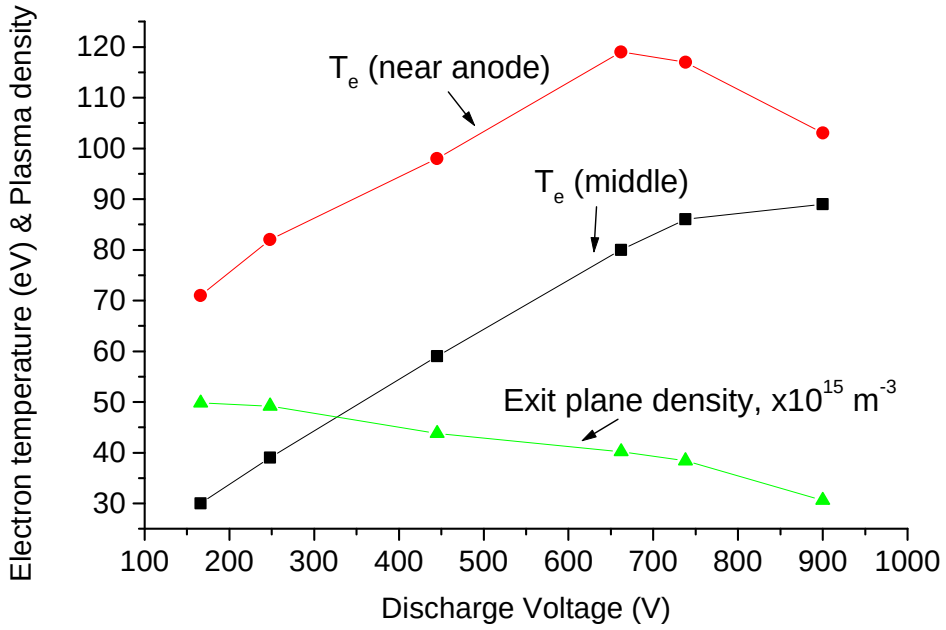

Figure 9. Electron temperature and plasma density at the exit plane dependent on the discharge voltage.

The calculations show that the plasma properties (density and electron temperature) depend strongly on the discharge voltage. An example is shown in Fig. 9 where electron temperature and plasma density are plotted. One can see that the electron temperature generally increases with discharge voltage, while plasma density decreases in the high voltage case. Near the anode plane the electron temperature has a non-monotonic behavior as shown in Fig.9. According to the model (Sec. II, Eqs. 1-5) the ionization rate proportional to the electron density and therefore decreases when electron density decreases. Thus one can expect that there is a trade off between ion current fraction increase due to electron temperature increase and ion current fraction decrease due to electron density decrease. This in turn leads to non-monotonic dependence of the thruster (anode) efficiency with discharge voltage. This trend is shown in Fig. 10 where the experimental results (Ref. 8) are also shown. It can be seen that the model predicts peak of efficiency similar to experiment.

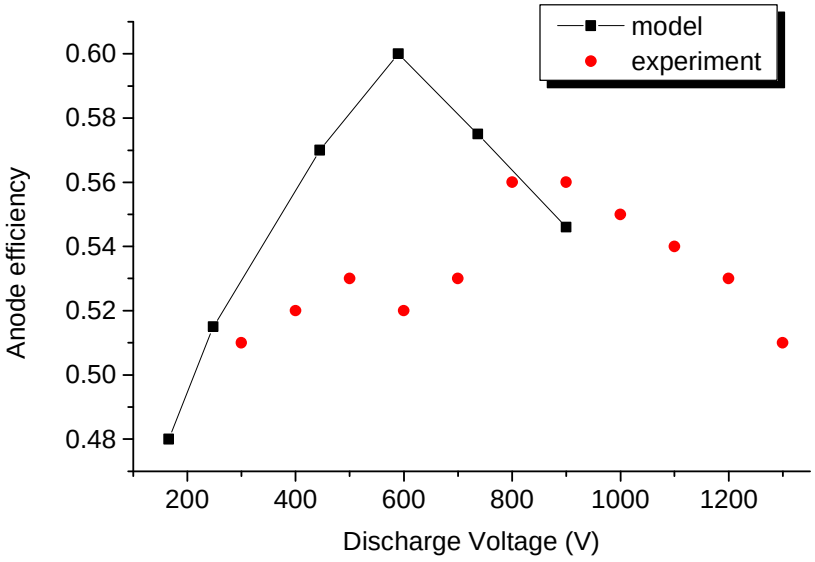

Fig. 10. *Efficiency dependence on the discharge voltage and comparison with experiment. Experimental data are taken from Ref. 8.*

IV. Quasi-1D model of the anode layer

It was shown in the previous sections that the effect of the sheath expansion in the acceleration channel may be very significant in the case of a high voltage TAL. It affects mainly the cross sectional area of the quasi-neutral plasma. Therefore the question is how sheath expansion may affect the parameter distribution in the quasi-neutral anode layer. To study this effect, we developed a simplified quasi-1D model of the discharge in crossed ExB fields. The original model of this discharge was developed by Zarinov and Popov.[3] Recently, a modified version of that model that took into account plasma-wall interactions by introducing a detailed electron energy equation was developed by Choueiri.[7] We present here a similar model in which we adopt the formulation of Refs. 3,7 except that sheath expansion in the acceleration region is taken into account. We take into account the effect of sheath expansion, as it occurs in a high power TAL. In this case, the current density in the quasi-neutral region will vary along the channel. The sheath near the channel wall will be quickly established with a time scale of about the

plasma frequency and therefore a steady state sheath will be considered. In this case, the cross sectional area A(x) is varied along the channel. We start with the following set of equations:

$$A\frac{dj_x}{dx} + j_x\frac{dA}{dx} = e\nu_{iz}n_eA \quad \text{..... (15)}$$

$$j_x = \mu_\perp(en_e\frac{d\varphi}{dx} - \frac{d(n_eT_e)}{dx}) \quad \text{..... (16)}$$

$$n_e = n_i = \frac{j_i(x)}{e\sqrt{\frac{2e(\varphi_a - \varphi)}{M}}} \quad \text{..... (17)}$$

$$\mu_\perp = \frac{e}{m_e\nu_e}\cdot\frac{1}{1+(\omega_e/\nu_e)^2} \quad \text{..... (18)}$$

where $\mu_\perp$ is the classical cross field mobility, $j_i(x)$ is the ion current dependent on the cross section, j_x is the electron current, ν_{iz} is the ionization frequency, ν_e is the electron collision frequency and ω_e is the electron cyclotron frequency. The cross section can be calculated as follows:

$$A(x) = \pi((R_2 - s)^2 - (R_1 + s)^2) \quad \text{..... (19)}$$

where R_1 and R_2 are inner and outer radii of the channel (see Fig.3), s is the sheath thickness (dependent on x) that can be calculated as follows in the case of the classical Langmuir sheath:

$$s = \frac{\alpha^{1/2}\varphi^{3/4}}{(en_eV_o)^{1/2}} \quad \text{..... (20)}$$

where $\alpha = (\frac{4}{9}\varepsilon_o)^{1/2}(\frac{2Ze}{m_i})^{1/4}$, en_eV_o is the ion flux to the wall and φ is the potential. The channel cross section at the exit plane A_o corresponds to the case of zero sheath thickness. In addition the simplified energy equation will be used: $T_e = \beta\varphi$, which is similar to Ref. 3.

Let us normalize the system of Eqs. (15-20). In order to compare results with Refs. 3,7 we will perform the same normalization: $\phi=\varphi/\varphi_a$, $\xi=x/l^*$, $n_e=n_e/n'$, $j_e=j_e/j^*$. The characteristic quantities can be defined as follows:

$$l^* = \sqrt{\frac{e\varphi_a}{\frac{\nu_{iz}}{\nu_e} m_e \omega_e^2}} \; ; n^* = \frac{j_{io}}{e\sqrt{\frac{2e}{M}\varphi_a}} ; \; j^* = e\nu_{iz} n^* l^* ; \bar{T} = \frac{T_e}{\varphi_a} ; \; \bar{A} = \frac{A(x)}{A_0}$$

The derivative of the channel cross section $A(x)$ can be calculated as follows:

$$\frac{1}{A}\frac{dA}{dx} = -\frac{2\frac{ds}{dx}}{\left(\frac{R_2^2 - R_1^2}{R_2 + R_1} - 2s\right)} \quad \text{..... (21)}$$

Finally the following normalized system of equations is obtained:

$$\frac{d\bar{j}}{d\xi} = \bar{n} \quad \text{..... (22)}$$

$$\bar{j} = \bar{n}\frac{d\phi}{d\xi} - \frac{d}{d\xi}(\bar{n}\bar{T}) \quad \text{..... (23)}$$

$$\bar{T} = \beta\phi \quad \text{..... (24)}$$

$$\bar{n} = \frac{\bar{A}}{\sqrt{1-\phi}} \quad \text{..... (25)}$$

The following particular case is considered: mass flow rate of 10 mg/s, discharge current of 10 A, Bismuth as the propellant, geometry of Ref. 9, R_1=6 cm and R_2=10 cm. In the calculation presented here we assume the constant electron temperature along the channel for simplicity (T_e=100 eV, see Sec. III). The effect of the sheath expansion on the anode layer potential profile is shown in Fig. 11. It can be seen

that sheath expansion strongly affects the potential profile. This effect leads to decrease of the anode layer thickness.

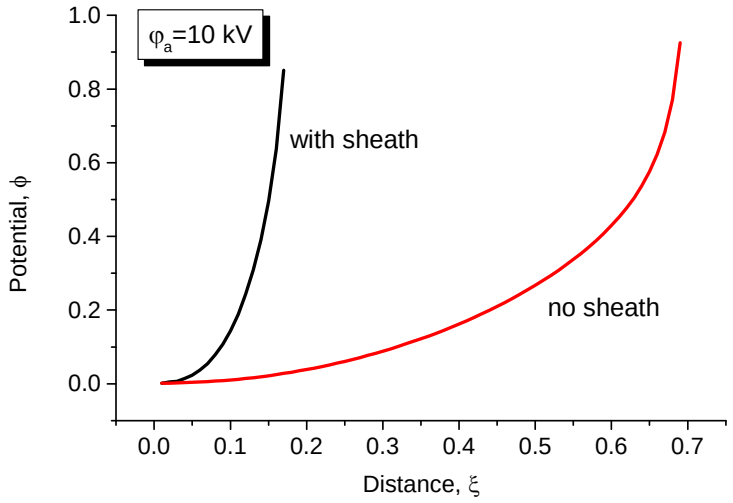

Fig. 11. *Potential profile with and without sheath expansion. Origin of the coordinate system (ξ=0) is located at the channel exit plane.*

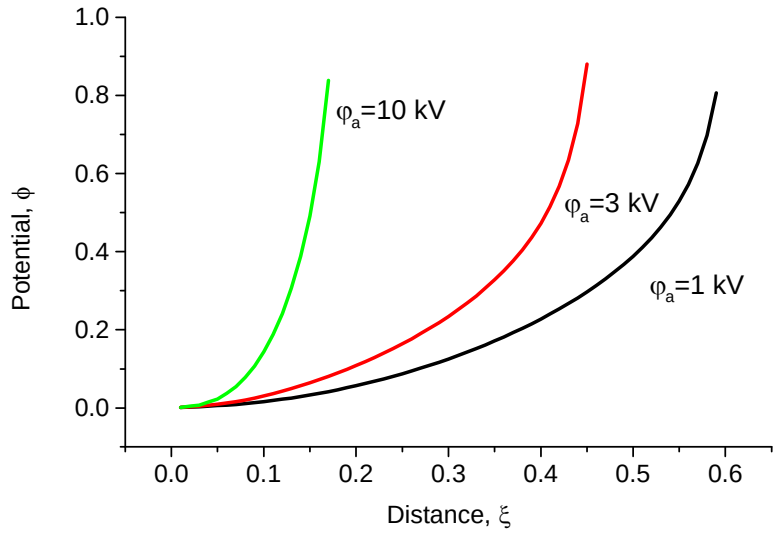

Fig. 12. *Potential profile with sheath expansion as a function of discharge voltage.*

The anode layer (acceleration channel) thickness dependence on the discharge voltage is shown in Fig. 12. One can see that the anode layer thickness significantly decreases with the discharge voltage increasing due to the sheath expansion effect. It is interesting to note that shrinking of the anode layer thickness is important as it leads to a smaller area of contact of the plasma with the walls and therefore smaller total erosion.

VI. Concluding remarks

In this paper, various aspects of the plasma flow in a high power thruster with anode layer (TAL) were studied. To this end, several models, such as a 2D hydrodynamic model, a quasi-1D model and a 1D PIC model were developed. In particular, plasma –wall interactions were studied in detail. One important aspect of those interactions is the sheath expansion in the acceleration channel. It was found that the high voltage sheath expands significantly and the quasi-neutral plasma region is confined in the middle of the channel. For instance, in the case of a 3 kV discharge voltage, the sheath thickness is about 1 cm, which is a significant portion of the channel width. It was found that the sheath expansion decreases the acceleration region length. This is an important effect as it leads to a smaller area of contact of the plasma with walls and therefore smaller total erosion. The single stage high voltage TAL (D-80) was studied. The model predicted a non-monotonic behavior of thruster efficiency with discharge voltage in agreement with experiment.

References

[1] R.J. Etherington and M.G. Haines, Phys. Rev. Lett., 14, 1019 (1965)

[2] G.S. Janes and R.S. Lowder, Phys. Fluids, 9, 1115 (1966)

[3] A.V. Zharinov and Yu.S. Popov, Sov. Phys. Tech. Phys., 12, 208 (1967)

[4] A.I. Morozov, Sov. Phys. Dokl., 10, 775 (1966)

[5] V.V. Zhurin, H.R. Kaufman and R.S. Robinson, Plasma Sources Sci. Technol., 8, 1 (1999)

[6] A.I. Morozov and V.V. Savelyev, in *Review of Plasma Physics*, Ed. By B.B. Kadomtsev and V.D. Shafranov (Consultant Bureau, New York, 2000), Vol. 21, p. 203.

[7] E. Choueiri, Phys. Plasmas, 8 5025 (2001)

[8] D.T. Jacobson, R.S. Jankovsky, V.K. Rawlin, D.H. Manzella, High Voltage TAL Performance, AIAA-2001-3777

[9] S. Tverdokhlebov, A. Semenkin, and J. Polk, AIAA Paper 2002-0348

[10] Keidar, M. and Boyd, I.D, "Effect of a Magnetic Field on the Plasma Plume from Hall Thrusters," *Journal of Applied Physics*, Vol. 86, 1999, pp. 4786-4791.

[11] A.E. Soloduchin and A.V. Semenkin, IEPC-2003-0204

[12] M. Keidar, I.D. Boyd and I.I. Beilis, Phys. Plasmas, v. 8, No. 12, 5315 (2001).

[13] I. I. Beilis and M. Keidar, Phys. Plasmas **5** 1545 (1998)

[14] V.S. Erofeev and L.V. Leskov in book "Physics and application of plasma accelerators", Ed. A.I. Morozov, Minsk, 1974 (in Russian)

[15] J. P. Bouef and L. Garrigues, J. Appl. Phys., 84, 3541 (1998).

[16] N. B. Meezan, W.A. Hargus, and M. A. Cappelli, Phys. Rev., E63 026410, 2001

[17] J.M. Fife and S. Locke, AIAA Paper-2001-1137

[18] E. Ahedo, P. Martinez-Cerezo, and M. Martinez-Sanches, Phys. Plasmas 8, 3058 (2001)

[19] A.I. Morozov and V.V. Savel'ev, Plasma Phys. Rep., 26, 2000, 219

[20] M.Keidar, I. Beilis, R L. Boxman and S. Goldsmith, J. Phys. D: Appl. Phys., 29, 1996, 1973.

[21] C. D. Child, Phys. Rev., **32** (1911) 492

[22] I. Langmuir, Phys. Rev., Ser. II 2 450 (1913)